Published online 12 May 2008

Nucleic Acids Research, 2008, Vol. 36, No. 10 ***e61***
doi:10.1093/nar/gkn246

Gel-based oligonucleotide microarray approach to analyze protein–ssDNA binding specificity

Olga A. Zasedateleva*, Andrey L. Mikheikin, Alexander Y. Turygin, Dmitry V. Prokopenko, Alexander V. Chudinov, Elena E. Belobritskaya, Vladimir R. Chechetkin and Alexander S. Zasedatelev

Engelhardt Institute of Molecular Biology, Russian Academy of Sciences, 32 Vavilov Street, 119991 Moscow, Russian Federation

Received August 6, 2007; Revised March 7, 2008; Accepted April 16, 2008

ABSTRACT

Gel-based oligonucleotide microarray approach was developed for quantitative profiling of binding affinity of a protein to single-stranded DNA (ssDNA). To demonstrate additional capabilities of this method, we analyzed the binding specificity of ribonuclease (RNase) binase from *Bacillus intermedius* (EC 3.1.27.3) to ssDNA using generic hexamer oligodeoxyribonucleotide microchip. Single-stranded octamer oligonucleotides were immobilized within 3D hemispherical gel pads. The octanucleotides in individual pads 5′-{N}$N_1N_2N_3N_4N_5N_6${N}-3′ consisted of a fixed hexamer motif $N_1N_2N_3N_4N_5N_6$ in the middle and variable parts {N} at the ends, where {N} represent A, C, G and T in equal proportions. The chip has 4096 pads with a complete set of hexamer sequences. The affinity was determined by measuring dissociation of the RNase–ssDNA complexes with the temperature increasing from 0°C to 50°C in quasi-equilibrium conditions. RNase binase showed the highest sequence-specificity of binding to motifs 5′-NNG(A/T/C)GNN-3′ with the order of preference: GAG > GTG > GCG. High specificity towards G(A/T/C)G triplets was also confirmed by measuring fluorescent anisotropy of complexes of binase with selected oligodeoxyribonucleotides in solution. The affinity of RNase binase to other 3-nt sequences was also ranked. These results demonstrate the applicability of the method and provide the ground for further investigations of nonenzymatic functions of RNases.

INTRODUCTION

Different types of DNA microarray-based approaches have been developed to identify sequence specificity for regulatory proteins (1–4). Among these are the ChIP-on-chip method, which enables identification of specific binding regions of a protein *in vivo*, and protein-binding DNA microarrays for *in vitro* profiling of DNA-binding sites.

Universal protein-binding DNA microarrays containing all possible single-stranded (ss) or double-stranded (ds) DNA sequences of a given length allow to determine *in vitro* the relative affinity of a protein to these sequences and remains the powerful tool in protein–DNA binding studies. Recently, microarrays containing all possible 8 and 10 bp DNA duplexes were used to define ds DNA specific sites for transcription factors and low-molecular-weight ligands (5,6). Morgan *et al.* (7) applied microarray containing all possible 6 nt single-stranded sequences to identify single-stranded motifs for a cold-shock protein binding.

We present an alternative microarray method for quantification of binding affinity of a protein to ssDNA. In contrast to most oligonucleotide microchip techniques based on 2D surface immobilization, we immobilize single-stranded octamer oligonucleotides within 3D hemispherical hydrogel pads (8–12). Immobilization of oligonucleotides within the pads allows us to quantify the affinity of a protein by measuring the complete set of $4^6 = 4096$ dissociation curves for protein–oligonucleotide complexes.

Guanyl-specific bacterial ribonuclease binase produced *by Bacillus intermedius* (EC 3.1.27.3) was used to develop further this approach. The earlier generation of 3D microarrays proved to be quite efficient for quantitative assessment of sequence specificity of low-molecular-weight compounds, ligands and proteins in their interactions with ssDNA, as well as dsDNA (8–11). Specific motifs found using these oligonucleotide microchips were also confirmed by alternative methods (10).

The RNase binase from *B. intermedius* is a member of a family of guanyl-specific enzymes that regulate cellular metabolism by catalyzing ssRNA degradation (13–18). The size of the substrate segment bound at the active site

*To whom correspondence should be addressed. Tel: +7 495 1359980; Fax: +7 495 1351405; Email: lana@biochip.ru

of guanyl-specific RNases, particularly for barnase, the closest homologue of RNase binase, was estimated to be three ribonucleotides in length (19,20). The mechanism of binase endoribonuclease activity towards ssRNA is similar to mammalian RNase A (14,15).

Molecular structures and molecular mechanisms of RNA cleavage are well established for many RNases, the affinity towards different substrate sequences for many of them is known in a broad general sense only. The comparative analysis of substrate sequence specificity is hampered not only by the need of massive combinatoric turnover of RNA sequences at the active site, but also by the essential cleavage activity of RNases. The latter difficulty may be partially resolved by using DNA substrate instead of RNA. Such replacement is commonly performed in X-ray studies of RNase–substrate complexes (21–23). Using NMR spectroscopy, it has been shown that the functional dynamics at the active site of ribonuclease binase, the mode of complexation and dissociation constant did not change significantly after DNA substrate substitution for RNA (24). There is additional interest in such a substitution, taking into account the possibility of additional functions of RNases, besides their primary enzymatic activity (25–27).

We analyzed the enzyme-binding affinity to all possible 6-nt DNA sequences by measuring the dissociation of the binase–DNA complexes under temperature increase in quasi-equilibrium conditions. The enzyme was covalently labeled with Texas Red fluorescent dye. To avoid possible influence of the dye on the active site, we developed a special protocol for binase labeling in the presence of 10-mer oligodeoxyribonucleotide 5′-GAGAGAGAGA-NH_2-3′, which was subsequently removed.

Using our microarray-based approach we demonstrate that RNase binase shows sequence-specificity of binding to 3-nt motifs 5′-G(A/T/C)G-3′ with the following order of preference: GAG>GTG>GCG. The affinity of RNase binase to other 3-nt sequences was also ranked. These results provide the ground for the further exploration of nonenzymatic functions of RNases.

MATERIALS AND METHODS

Oligonucleotides

Oligonucleotides were synthesized at 1 μmol scale using ABI 394 DNA/RNA Synthesizer (Applied Biosystems, Foster City, CA, USA) and standard phosphoramidite chemistry; 3′-C(7) amino modifier was purchased from Glen Research (Sterling, VA, USA). The octadeoxyribonucleotides used for the immobilization in the gel pads of generic microchip have the structure 5′-{N}$N_1N_2N_3N_4N_5N_6${N}-NH_2-3′, where $N_1N_2N_3N_4N_5N_6$ is one of $4^6 = 4096$ possible 6-nt sequences and {N} corresponds to equimolar mixture of four nucleotides A, T, G and C. Thus, the flanking positions {N} are degenerate.

Decadeoxyribonucleotide 5′-GAGAGAGAGA-NH_2-3′ was labeled with amine-reactive fluorescent Dye-2 (N-hydroxysuccinimide ester of 4,4-difluoro-5,7-dimethyl-4-bora-3a,4a-diaza-*s*-indacene-3-yl propionic acid) provided by Biochip-IMB (Moscow, Russia). Dye-2 is similar to Bodipy dyes (Invitrogen, Carlsbad, CA, USA) and has absorption/emission wavelengths $\lambda_{abs} = 500$ nm $\lambda_{em} = 512$ nm. Heptadeoxyribonucleotides 5′-TTGAGTT-NH_2-3′, 5′-TTGTGTT-NH_2-3′, 5′-TTGCGTT-NH_2-3′ and 5′-TTTTTTT-NH_2-3′ were labeled with amine-reactive fluorescent Dye-3 [N-hydroxysuccinimide ester of 3-(4,4-difluoro-1,3,5,7-tetramethyl-4-bora-3a,4a-diaza-*s*-indacene-2-yl) propionic acid] provided by Biochip-IMB. Dye-3 is also similar to Bodipy dyes (Invitrogen) and has absorption/emission wavelengths $\lambda_{abs} = 517$ nm and $\lambda_{em} = 522$ nm. To perform labeling, HPLC-purified oligonucleotides were dissolved in H_2O and cooled to 0–5°C. Dye-2 or Dye-3 dissolved in dry pyridine and cooled to 0°C were added to oligonucleotide water solution (molar ratio dye:oligonucleotide 5:1, volume ratio of solutions 1:1) and incubated at 0–5°C overnight. The mixture was diluted with 0.1 M TEAA buffer (pH 7.0), the excess of the dyes extracted with *n*-butanol, and the oligonucleotides were purified using HPLC.

The purity of the octadeoxyribonucleotides was controlled using MALDI-TOF mass-spectrometer COMPACT MALDI 4 (Kratos Analytical, Chestnut Ridge, NY, USA). The concentrations of the oligodeoxyribonucleotides were measured with spectrophotometer Jasco V-550 (Jasco, Japan) using extinction coefficient derived from nearest-neighbor model (28).

Generic microchip manufacturing

Generic microchips were manufactured according to the IMAGE chip technology (12,29).

The generic microchip consisted of an array of 3D hydrogel pads of hemispherical shape automatically spotted on hydrophobic glass slide (3 in. by 1 in.; Cell Associate, Inc., The Sea Ranch, CA, USA) by a pin robot QArray (Genetix). Octamers with embedded 4096 possible 6-nt sequences extended with degenerated single nucleotides at both ends were covalently immobilized in the gel pads. Thus, each 3D hydrogel pad of the generic microchip contained octadeoxyribonucleotides with a unique inner 6-nt sequence. The pads were 0.2 nl in volume and 80 μm in diameter. The distance between neighbouring pads was 250 μm. The total area of the array was 17.8×15.9 mm^2.

Since the manufacturing of IMAGE generic microchips involved a combined step of photo-induced gel polymerization and DNA immobilization, immobilized oligonucleotides were uniformly distributed within the volume of each hydrogel pad (12). The efficiency of oligonucleotide immobilization inside the gel pads was ~50% in accordance with earlier results (12), while the final concentration of immobilized oligonucleotides within the gel pads was about 25 μM.

Covalent labeling of RNase binase

Wild-type binase was expressed in pMT416 bacterial expression vector (Novagen, Madison, WI, USA) in *Escherichia coli* strain BL21(DE3)[pLysS] cells (Novagen) and purified by phosphocellulose chromatography as described earlier (30,31).

To detect the RNase binase interaction with oligonucleotides immobilized in the gel pads of generic microchip,

the enzyme was covalently labeled with Texas Red (TR) sulfonyl chloride fluorescent dye (Molecular Probes, Eugene, OR, USA) (absorption/emission wavelengths $\lambda_{abs} = 588$ nm and $\lambda_{em} = 601$ nm) (32). To prevent covalent binding of the amine-reactive dye TR to amino acids in the active center, the labeling of binase was performed in the complex with fluorescently labeled 10-mer 5′-GAGA GAGAGA-3′. This 10-mer was labeled with another fluorophore, Dye-2, similar to Bodipy dyes (absorption/emission wavelengths $\lambda_{abs} = 500$, $\lambda_{em} = 512$) to control the completeness of removal of the 10-mer from TR-labeled enzyme.

To perform covalent labeling, binase was dissolved in 100 µl of 0.1 M $NaHCO_3$, pH 8.5, to 10^{-4} M (32). Concentrated water solution of fluorescently labeled 10-mer was added to RNase binase solution (molar ratio oligonucleotide:enzyme 5:1). The mixture was incubated at 0°C for 10 min for binding. Solution of TR sulfonyl chloride in dimethylformamide (20 mg/ml) cooled to 0°C was added to binase–oligonucleotide complex (molar ratio dye:enzyme 100:1). The enzyme was labeled at 0°C for 4 h in the dark. The labeled enzyme was purified from oligonucleotide and the excess of unreacted molecules of TR fluorophore by gel filtration using QAE Sephadex A-25 (Pharmacia Fine Chemicals AB, Uppsala, Sweden). According to absorbance measured from 700 to 190 nm, fluorescently labeled 10-mer was removed completely. The concentration of the enzyme was measured by absorption at 280 nm assuming that the extinction coefficient equals 27 411 $M^{-1} cm^{-1}$ (31).

The extent of protein modification was assessed by MALDI-TOF mass-spectrometry and absorption spectrum at 595 and 280 nm and found to be 0.5 dye residue per enzyme molecule.

Measurements of dissociation curves of complexes between TR-labeled binase and oligonucleotides of generic microchip

All measurements on generic microchips were performed in real time by an automated research custom-made fluorescent microscope (Biochip-IMB) with 10×10 mm^2 field, mercury lamp as the excitation source and the filter set for TR dye ($\lambda_{ex} = 580$ nm and $\lambda_{em} = 630$ nm). The microscope was equipped with a CCD camera (SenSys, Roper Scientific, Tucson, AZ, USA), a Peltier thermotable with temperature controller (Melcor, Trenton, NJ, USA), and a scanning system consisting of a two-coordinate table, step-wise motor, and motion controller (Newport, Irvine, CA, USA).

The generic microchip consisted of four fields. Two fields comprised 972 gel pads each, including 36 gel pads containing immobilized markers and four empty gel pads in each field. Fluorescently labeled oligonucleotide gel-5′-NH-TTTTTTTT-NH-TR immobilized within corresponding gel pads at final concentration 6 µM was used as the marker. Two other fields consisted of 1152 gel pads each, including 36 gel pads per field containing immobilized markers. The microchip was scanned field by field at each temperature point. Each field was exposed for 7 s, and the whole microchip (four fields) was scanned in 55 s. The microscope was equipped with a computer and Imagel Research software developed in our laboratory (33) to operate the experiments and record fluorescent signals and images of the whole generic microchip at each temperature point. Recording of the whole image at each temperature enabled us to recalculate the whole set of dissociation curves if needed.

Binding of TR-labeled binase with 4096 octadeoxyribonucleotides immobilized in gel pads of the generic microchip was performed at 0°C for 4 h. Binding and subsequent dissociation of the formed complexes were carried out in 50 µl chamber. Both processes were performed in Buffer A (0.1 M NaCl, 50 mM Tris–HCl, pH 6.5, 1 mM EDTA) containing 2×10^{-5} M of TR-labeled binase. The dissociation curves were recorded for all pads of the microchip with the temperature increase from 0°C to 65°C at the rate of 1°C/30 min. According to the kinetic curves of binding at 0°C between TR-labeled binase and oligonucleotides of generic microchip, the time of about 30 min was sufficient for fluorescent signals to reach 90% saturation. Therefore, the whole curve of the dependence of fluorescence intensity on temperature was obtained in quasi-equilibrium conditions reached at every temperature step.

Data processing

Fluorescence signals from individual pads were processed using ImaGel Research software. Fluorescent image of each gel pad of the microchip was surrounded by inner and outer circular frames: inner frame enclosed the gel pad itself, while outer frame enclosed the background around it. Intensity of fluorescence, J, from a microchip gel pad was defined according to the equation:

$$J = \frac{In - Out}{Out - Dc} - \frac{1}{8}\sum_{i=1}^{8}\left(\frac{In - Out}{Out - Dc}\right)_{ref_i} \quad \mathbf{1}$$

where In is the average intensity of fluorescence inside the inner frame occupied by the gel pad, Out is the average intensity of fluorescence in the space between the inner and outer frames occupied by the outer region of the gel pad, Dc is the average noise signal inside the inner frame produced by dark current at zero illumination intensity, while the counterpart expression with subscript 'ref' corresponds to the signals from empty gel pads without immobilized oligonucleotide probes.

All experiments on the measurements of dissociation curves for binase-ssDNA complexes were repeated twice on two different generic microchips. The subsets of 3963 and 3891 melting curves were selected for subsequent analysis according to the criteria developed earlier (10): the pads whose initial signals were below 20% of the average initial signals for the whole set were excluded from further consideration, and they constituted up to 5% of all curves. The filtered curves were approximated by least squares method using the following fitting equation described earlier (10) to obtain the set of dissociation temperatures, T_D:

$$J(T) = A + \frac{B}{1 + \left(\frac{T}{T_D}\right)^N} \quad \mathbf{2}$$

where $J(T)$ is the measured intensity of fluorescence, T is temperature (K), T_D is dissociation temperature (K), $A+B$ is initial intensity, A is final intensity, N is fitting parameter. After fitting procedure, the resulting set of T_D values was converted to centigrees. Dissociation temperature, T_D, for the complexes between RNase binase and oligonucleotides was defined as a temperature at which half of the complexes in a microchip gel pad are in nondissociated state in equilibrium thermodynamic conditions. In our conditions, it may also be approximately assessed by the temperature at which the fluorescence intensity is half of the intensity at 0°C.

In our microarray experiments, the enzyme (1 nmol) was taken in excess with respect to the total amount of immobilized oligonucleotides (2×10^{-2} nmol), or $C_p \cdot V_{chamber} >> C_{imm} \cdot V_{pad} \cdot n$, where C_p is the concentration of protein in applied solution, C_{imm} is the concentration of immobilized oligonucleotides, $V_{chamber}$ and V_{pad} are the volumes of the microchip chamber and a single microchip gel pad correspondingly, n is total amount of gel pads. Thus, the concentration of free protein can be assumed to be constant and does not depend on concentration of protein–ssDNA complexes at each temperature point.

Taking into account this condition and in accordance with the mass action law the equilibrium binding constant, $K(T)$, for the formation of protein–ssDNA complexes inside a microchip gel pad can be expressed as follows:

$$K(T) = \frac{C_{complex}(T)}{C_p(C_{imm} - C_{complex}(T))} \quad \mathbf{3}$$

where T is temperature (°K), C_{imm} is the concentration of immobilized oligonucleotides, C_p is the concentration of binase in applied solution, and $C_{complex}(T)$ is the concentration of binase–oligonucleotide complexes.

Dissociation temperature, T_D, for the complexes between RNase binase and oligonucleotides is defined as the temperature at which half of the complexes in a microchip gel pad are in nondissociated state in equilibrium thermodynamic conditions, or $C_{complex} = C_{imm}/2$. Thus, at dissociation temperature $T = T_D$, the equilibrium binding constant from Equation (3) can be expressed as follows:

$$K|_{T=T_D} = \frac{1}{C_p} \quad \mathbf{4}$$

According to van't Hoff equation,

$$K(T) = \exp\left(\frac{-\Delta F(T)}{RT}\right) \quad \mathbf{5}$$

where ΔF is the change in binding free energy and R is universal gas constant. Taking into account the relationship (4), we obtain the following relationship between the change in binding free energy and dissociation temperature:

$$\Delta F|_{T=T_D} = R \cdot T_D \cdot \ln C_p \quad \mathbf{6}$$

This relationship shows that in the process of equilibrium dissociation the higher the dissociation temperature, T_D, the higher the change in binding free energy. Due to this relationship, the binding constants keep the same value, $1/C_p$, at dissociation temperatures $T = T_D$, for all complexes between the protein and oligonucleotides of generic microchip [Equation (4)]. The relationship (6) also shows that T_D can be used for quantitative assessment of binding affinity.

Fluorescence anisotropy measurements

Measurements of intensities of polarized fluorescence, $I_{||}$ and $I_{\perp}$, were performed using a Cary Eclipse fluorescence spectrophotometer (Varian Australia) equipped with a manual polarizer and single cell holder with temperature control. The excitation and emission wavelengths were 510 and 530 nm, respectively, with 10 nm band-pass and an integration time 30 s. Target heptadeoxiribonucleotides were labeled with Dye-3, which is similar to Bodipy dyes (absorption/emission wavelengths $\lambda_{abs} = 517$, $\lambda_{em} = 522$, molecular mass of the dye residue of a modified oligonucleotide is 303.13 Da). Each Dye-3 labeled heptamer was titrated with increasing concentration of protein, with the total [protein] >> [oligonucleotide] at each titration point. The titration was carried out at 20°C, at equilibrium conditions. After each addition, the cuvette (1 cm × 1 cm) with sample was rotated gently, equilibrated at the required temperature for 5 min and polarized intensities of fluorescence were measured. All titrations were performed in buffer A. Initial concentration of oligonucleotide was 10 nM, volume 1 ml. In total, 60 µl of protein solution was added. The decrease in oligonucleotide concentration during the titration as well as protein absorption were taken into account in the analysis of the data and computation of the values of anisotropy of fluorescence.

Fluorescence anisotropy data analysis

Equilibrium binding curves obtained using fluorescence anisotropy were fit to a standard single-site isotherm usable when [protein] >> [oligonucleotide] (34):

$$A(C_p) = A_0 + \frac{(A_{max} - A_0) \cdot C_p \cdot K}{1 + C_p \cdot K}$$

where A is fluorescence anisotropy, A_0 is fluorescence anisotropy of oligonucleotide in the absence of the protein in solution, A_{max} is the value of fluorescence anisotropy when all oligonucleotides are in bound state with the enzyme, C_p is the total binase concentration at each point in the titration, and K is the association constant for binase–DNA binding. Fitting was performed using the program Origine 6.1 (OrigineLab Corp., Northampton, MA, USA). Fitting parameters were K, A_0 and A_{max}.

RESULTS

The affinity of binase binding to all possible 6 nt ssDNA sequences was quantitatively assessed via measurements of fluorescence signals from the complexes formed between ssDNA and TR-labeled binase. To avoid the inactivation of binase during modification, its active site was protected

by temporary binding of 10-mer oligodeoxyribonucleotide 5′-GAGAGAGAGA-NH_2-3′, which was removed after the reaction (see Materials and methods section).

Figure 1A shows the image of generic microchip recorded after 4 h of incubation at 0°C with TR-labeled binase. Most gel pads have visible fluorescence demonstrating strong binding of TR-labeled binase to corresponding immobilized oligonucleotides. The fluorescence intensities differ depending on their sequences.

Figure 1B shows examples of dissociation curves for eight complexes between the enzyme and oligonucleotides of generic microchip. Because of the variations of the affinity of binase to different sequences, the corresponding complexes showed different stability. Dissociation temperatures vary from 26.5°C for octadeoxiribonucleotide containing inner TCTGCC 6-nt sequence to 48.3°C for octadeoxiribonucleotide containing inner AGTGTG 6-nt sequence.

Figure 1C shows the distribution of dissociation temperatures of binase–oligonucleotide complexes. Dissociation of the complexes occurs below 50°C, while the mean value of dissociation temperature for all binase–oligonucleotide complexes is 40.2°C. It should be noted that the denaturation temperature of binase in similar physico-chemical conditions is 55°C, and the conformation of the enzyme remains stable up to 50°C (31,35). Thus, the dissociation temperatures determined in this work characterize the binding affinity of RNase binase in its native form.

All measurements of dissociation curves for binase–ssDNA complexes were repeated twice and the results were reproducible. The data presented below correspond to averages of two experiments. Table 1 (Supplementary Material) contains the values of the dissociation temperatures and the intensities of fluorescence at 40°C for the complexes between TR-labeled binase and oligonucleotides of the generic microchip.

Figure 2A shows a computer representation of the dissociation temperatures measured for the complexes between TR-labeled binase and octadeoxyribonucleotides of generic microchip. The most stable binase–oligonucleotide complexes are found in six rectangular regions. Three of these regions arranged in columns correspond to common motif 5′-NG(A/T/C)GNN-3′, where N is one of the four nucleotides. The other three rectangular regions arranged in rows correspond to the same 5′-NNG(A/T/C)GN-3′ common motif shifted by one nucleotide to the right.

The effective dissociation temperatures for shorter motifs were obtained as the mean values over all hexamer sequences containing a given shorter motif and summarized in Figure 2B–F. G was found to be the best mononucleotide motif, GA, AG, GG as well as GT, TG, GC and CG were found to be the best dinucleotide motifs, GAG, GTG and GCG the best 3-nt motifs, NG(A/T/C)G, G(A/T/C)GN the best 4-nt motifs and NG(A/T/C)GN G(A/T/C)GNN and NNG(A/T/C)G the best 5-nt motifs. These results demonstrate that starting from the length of four bases the most specific motifs are organized by addition of degenerated nucleotides to the ends of 5′-G(A/T/C)G-3′ motifs, thus revealing the

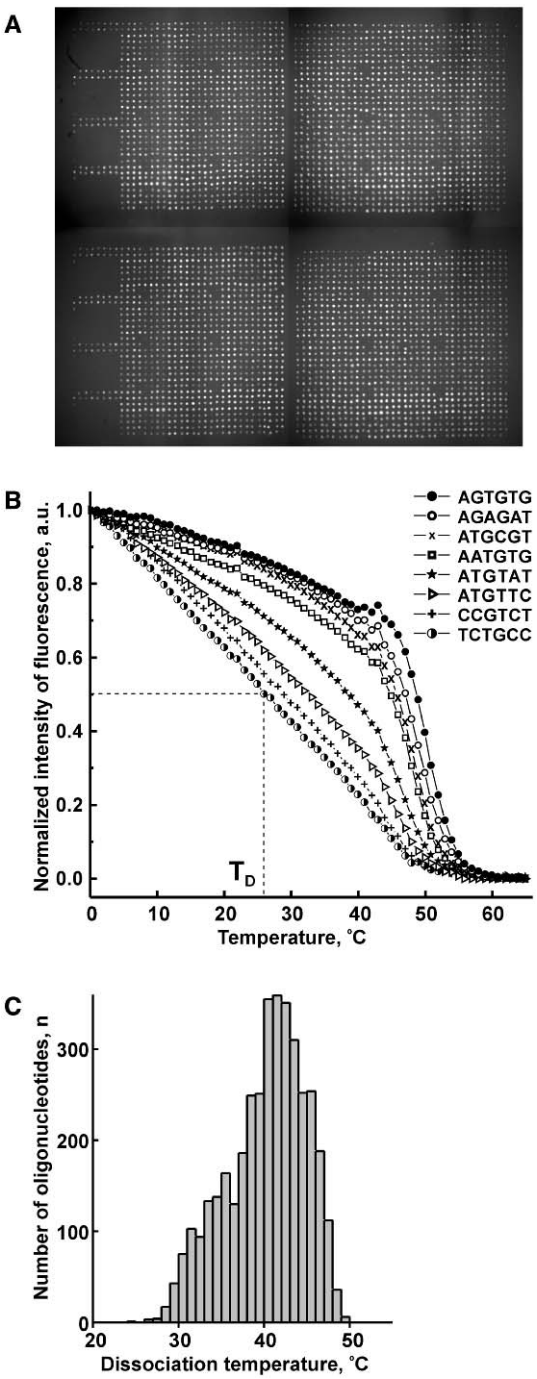

Figure 1. Interaction of TR-labeled RNase binase with octadeoxyribonucleotides immobilized on generic microchip. (**A**) Overview of generic hexamer deoxyribonucleotide microchip after binding with TR-labeled RNase binase from *B. intermedius*. Each octadeoxyribonucleotide immobilized in a given gel pad contains a fixed hexamer $N_1N_2N_3N_4N_5N_6$ in the middle of 5′-{N}$N_1N_2N_3N_4N_5N_6${N}-3′ sequence, where variable nucleotides {N} at 5′- and 3′-ends are A, C, G and T in equal proportions. (**B**) Normalized dissociation curves for the complexes between TR-labeled RNase binase and eight octadeoxyribonucleotides immobilized on generic microchip. The complexes are characterized by different binding affinity. Dotted lines illustrate the approximate assessment of T_D value for 5′-NTCTGCCN-3′ octadeoxyribonucleotide. Sequences of the inner 6-nt long sequences of the immobilized octadeoxyribonucleotides are shown in the upper right corner. (**C**) Distribution of the number of binase–oligonucleotide complexes plotted against their dissociation temperatures.

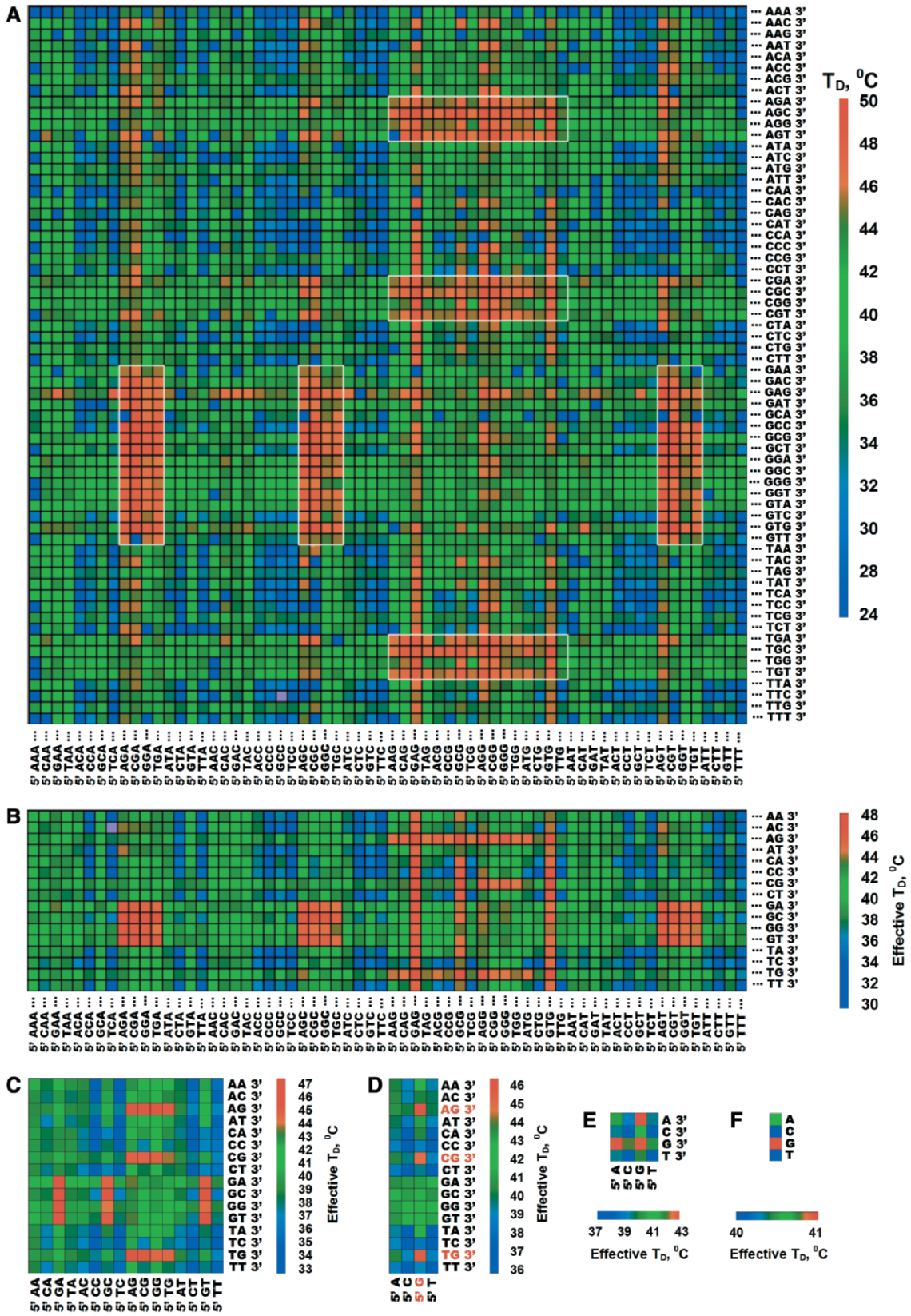

Figure 2. Computer representation of dissociation temperatures, T_D, for complexes between TR-labeled RNase binase and octadeoxyribonucleotides of the generic microchip. Each hexanucleotide sequence should be read by combining its 5′-half in the column with 3′-half in the row. Set (**A**) refers to the initial data measured with generic hexamer microchip and averaged over two experiments. (**B–F**) represent effective dissociation temperatures for all possible sequences of the length 5, 4, 3, 2 and 1 nt, correspondingly. The effective dissociation temperatures for sequences shorter than 6 nt were obtained as the mean values over T_D values for all 6-nt sequences containing a given shorter motif. For instance, the value for the sixth data point in the upper row in (B) was obtained as the mean value for all hexamers from (A) containing sequence 5′-CCAAA-3′; the value for the second element in the bottom row of (D) is the mean for all hexanucleotides containing sequence 5′-CTT-3′, etc. The re-arrangement of figure (A) into (B–F) was carried out using VirtualChip software developed in our laboratory. Color scales of T_D values are shown next to corresponding matrices.

distinct sequence-specificity of the binase towards these motifs. This is in agreement with earlier observations (14,19,20), which demonstrated that RNase binase is guanyl-specific and that the length of the substrate fragment in the active site is 3-nt, similarly to other guanyl-specific ribonucleases. Our data also provide additional information on the sequence-specificity of binase–ssDNA binding.

Similar results were obtained by analyzing the values of fluorescent intensities measured at 40°C for TR-labeled binase–ssDNA complexes formed in microchip gel pads (Figure 3A–F). Figure 3A shows the same six rectangular regions corresponding to 5′-NG(A/T/C)GNN-3′ and NNG(A/T/C)GN-3′ as the common specific motifs shifted by one nucleotide within the hexamer. Figure 3B–F helps to visualize the 5′-G(A/T/C)G-3′ sequence as the binase-specific 3-nt binding motif. The results obtained at 40°C are in good agreement with the results obtained using the dissociation temperatures and strongly suggest that RNase binase did not undergo denaturation within the temperature range used in the melting experiments, from 0°C to 50°C. These results also demonstrate the possibility to study the binding specificity of proteins to oligonucleotides immobilized on generic microchip at a constant temperature. It has to be noted that in this case it is necessary to have preliminary data on the average dissociation temperature of the complexes.

The impact of the flanking nucleotides on the affinity of RNase binase to 5′-G(A/T/C)G-3′ motif is shown in Figure 4. The mean dissociation temperatures for hexanucleotides containing G(A/T/C)G motifs at their ends (i.e. one nucleotide from the end of the immobilized octamer) is 1–2°C lower then for those containing G(A/T/C)G motifs in the middle. It should be noted that mean dissociation temperatures for hexanucleotides with G(A/T/C)G motifs near their 3′-ends is lower then for those containing G(A/T/C)G motifs near 5′-ends. This could be explained by the presence of amino-linker at the 5′-end of immobilized octadeoxyribonucleotides. Thus, the specificity of RNase binase towards its consensus sequence reaches its maximum when the G(A/T/C)G is located two nucleotides from the end of immobilized octamer.

Figure 5 shows the affinity of RNase binase to all possible 3-nt sequences flanked by at least two nucleotides within octanucleotide sequence and ranked in decreasing order according to the values of effective dissociation temperatures. Effective T_D values for GAG, GTG and GCG sequences are at least two degrees higher than for other triplets. In general, RNase binase shows higher affinity towards purine-rich 3-nt sequences as compared with pyrimidine-rich 3-nt sequences. The affinity of RNase binase to 3-nt homonucleotide sequences ranks in the order GGG > AAA > CCC ≥ TTT.

To validate our results obtained using the microarray approach, the binding affinities of unlabeled RNase binase towards TTG(A/T/C)GTT 7-nt sequences were measured using fluorescence anisotropy method and compared with the binding affinity of the enzyme towards TTTTTTT 7-nt homonucleotide sequence. We used oligonucleotides labeled at their 3′ ends with an analog of Bodipy dye. According to the equilibrium titration curves shown in Figure 6, the estimated values of association constants for TTGAGTT, TTGTGTT and TTGCGTT oligodeoxyribonucleotides were found to be $(54\,000 \pm 8000)\,M^{-1}$, $(56\,000 \pm 13\,000)\ M^{-1}$ and $(47\,000 \pm 7000)\,M^{-1}$, correspondingly, which are identical within the limits of error. For comparison, the association constant measured earlier for d(GCAG) was found to be between 20 000 and $10\,000\,M^{-1}$ (24). Figure 6 also shows that the enzyme exhibited significantly lower extent of affinity towards TTTTTTT sequence than towards TTG(A/T/C)GTT sequences. Table 2 (Supplementary Material) contains the data for titration curves. As shown using the microarray approach, the enzyme exhibits the highest sequence-specificity in interaction with G(A/T/C)G 3-mers flanked by 2 nt at both ends and one of the lowest affinity towards TTT 3-mer flanked by 2 nt from both ends (see Figure 5 for comparison). Thus, the difference in binding affinities of RNase binase towards highly specific triplets and a nonspecific one was confirmed by direct measurements of their interaction with unlabeled protein in solution.

DISCUSSION

Our microarray-based analysis proves that in the temperature range 0–50°C corresponding to the native form of RNase binase the enzyme binds with the highest affinity to ssDNA motifs 5′-G(A/T/C)G-3′ incorporated within the longer strands with degenerate nucleotides in their 5′- and 3′-flanking regions. The order of preference is GAG > GTG > GCG. Measurement of the affinity of RNase binase to all possible 3-nt sequences indicates that generally it displays the highest affinity towards purine-rich 3-nt sequences and the lowest towards pyrimidine-rich 3-nt sequences. Its affinity towards 3-nt long homonucleotide sequences is GGG > AAA > CCC ≥ TTT. These results on sequence-specificity of binase towards 3-nt ssDNA sequences correlate with the published data on the rate of enzymatic cleavage of Np–Np bonds in ssRNA directly related to the type of nucleoside at the 5′-end of the phosphodiester bond to be split. As shown by Bulgakova *et al.* (15), the enzyme preferentially splits Gp–Np and Ap–Np bonds in ssRNA, with the order of preference Gp–Np > Ap–Np, displaying significantly lower activity towards Pyrp–Np bonds. In a later review, sequence-specificity of RNase binase towards ss RNA was summarized as G > A > pyrimidines (14).

The affinity of RNase binase towards 3-nt long homodeoxyribonucleotides determined in this work also correlates well with the published data on the rate of cleavage of homo-polyribonucleotides by the enzyme. Yakovlev *et al.* (36) demonstrated that the rate of hydrolysis of purine polyribonucleotides is 3–4 order of magnitude higher than that of pyrimidine ones.

The high-affinity motif found in this work is also in agreement with the previous observations on 3-nt length of the substrate segment bound at the active site. These data were obtained during the study of catalytic activity of microbial ribonucleases towards ssRNA (19,20).

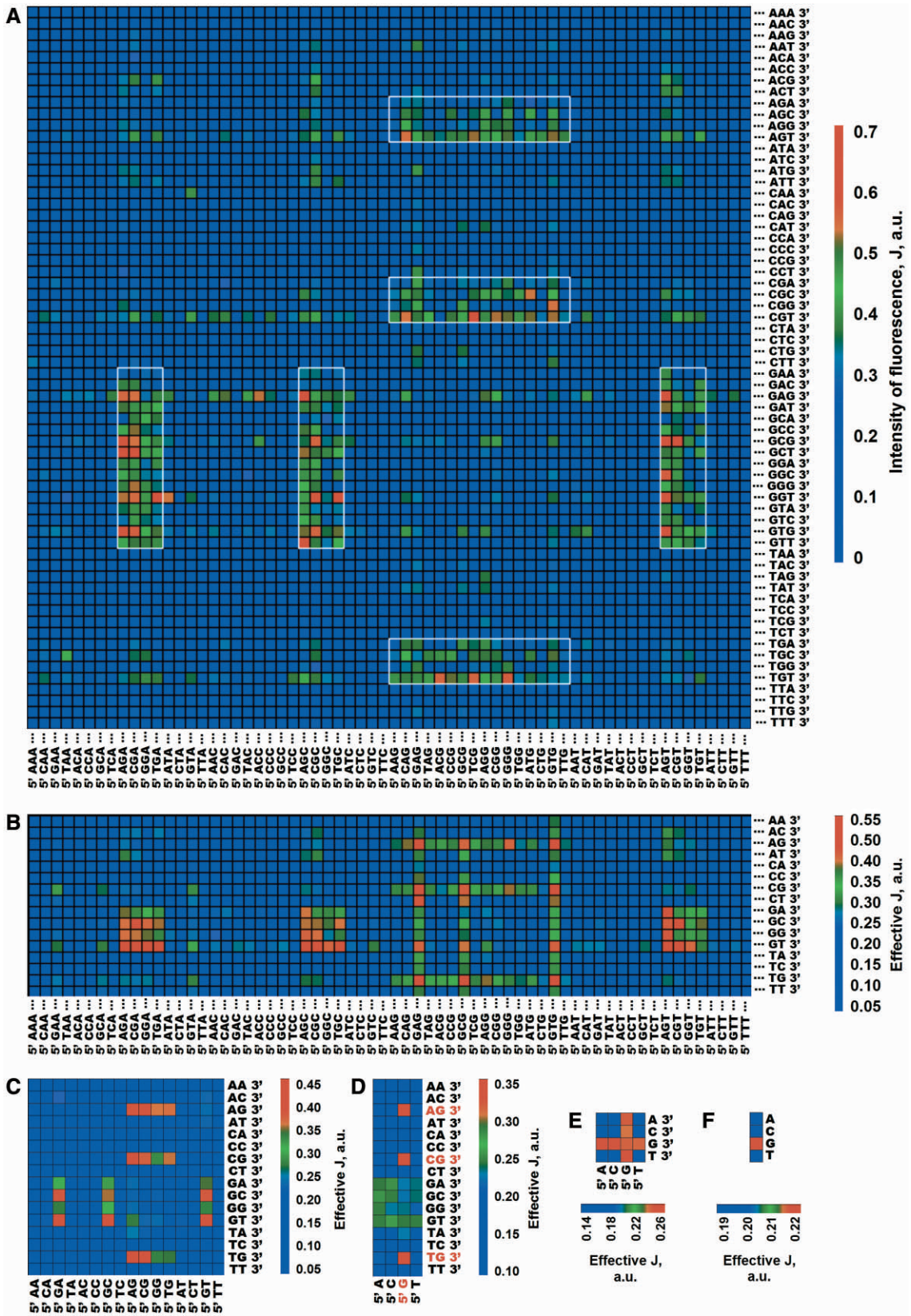

Figure 3. Computer representation of fluorescence intensities, *J*, at 40°C, for complexes of TR-labeled RNase binase with octadeoxyribonucleotides of the generic microchip. Each hexanucleotide sequence should be read by combining its 5′-halve in the column with 3′-halve in the row. Set (**A**) refers to the initial data measured with generic hexamer microchip and averaged over two experiments. (**B–F**) represent effective values of fluorescence intensities for all possible sequences of the length 5, 4, 3, 2 and 1 nt, correspondingly. (B–F) were obtained from the data shown in (A) as described in the legend to Figure 2.

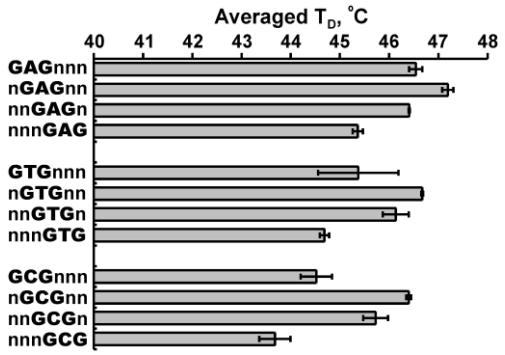

Figure 4. Dissociation temperatures of binase–oligonucleotide complexes plotted against different positions of GAG, GTG or GCG motifs within inner hexanucleotide sequences of immobilized octadeoxyribonucleotides. In each of two experiments, the data sets for 63–64 hexanucleotide sequences were used to calculate mean T_D value for the each position. The histogram indicates the calculated mean T_D values averaged over two experiments. The bars indicate the margin of error of T_D. All sequence data refer to the inner hexanucleotide sequences of immobilized octadeoxyribonucleotides.

Using fluorescence anisotropy method, we determined the binding affinities of unlabeled enzyme towards highly specific sequences TTG(A/T/C)GTT, which were found to be approximately the same and significantly higher than that for nonspecific oligodeoxyribonucleotide TTTTTTT.

In our microarray analysis, we used fluorescently labeled enzyme. To avoid possible influence of the dye on the active site of the enzyme, we developed a special protocol for labeling: the enzyme was labeled in the presence of sequence-specific oligodeoxyribonucleotide, which was removed after the reaction. According to the mass-spectrum, the majority of modified molecules contained only one covalently attached fluorophore (data not shown).

The specificity of hydrolytic activity of nucleases vary widely, with some of them being strictly specific to DNA or RNA substrates and to single-stranded or double-stranded nucleic acids. The activity of other enzymes is rather broad and can be directed against both RNA and DNA, as well as single-stranded and double-stranded nucleic acids (37). The strong binding of an enzyme to single-stranded DNA or RNA often implies that it can destabilize double-stranded DNA or RNA upon binding [for discussion and further references see ref. (10)]. Indeed, our preliminary data on melting of gel-immobilized duplexes in the presence of binase indicate the destabilization of dsDNA by the protein (unpublished data).

Besides the catalysis of RNA degradation, ribonucleases display other biological activities, some of which seem to be independent of their ribonucleolytic action. Many of them exhibit cytotoxic action, triggering apoptotic events, and therefore offer therapeutic opportunities for cancer treatment (25–27,38–41). Thus, onconase, an amphibian homolog of mammalian RNase A, selectively target tumor cells and is currently in phase III of human clinical trials as a chemotherapy treatment (25). *Bacillus intermedius* RNase (binase) was shown to kill preferentially mammalian cells expressing ras-oncogene (40). The complete network of molecular interactions responsible

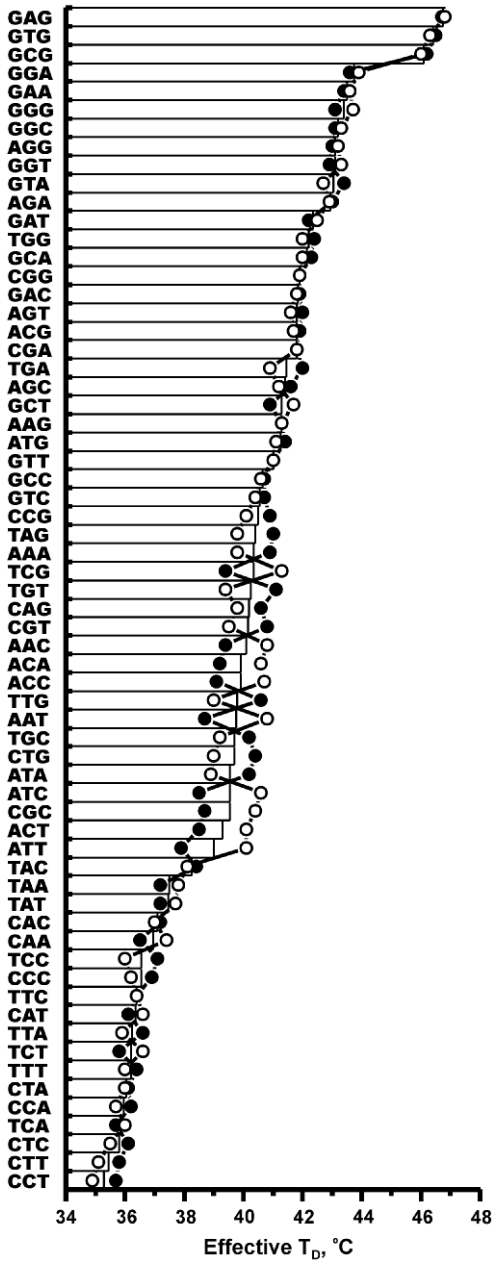

Figure 5. Affinity of RNase binase to all possible 3-nt sequences flanked by at least 2 nt from each end. The effective T_D values were obtained as the mean values over experimentally measured T_D values for the complexes between binase and immobilized 8-mers with inner hexanucleotide sequences of the latter containing a given 3-nt sequence in one of the middle positions. The effective T_D values obtained in two different experiments are shown using filled and open circles, correspondingly. The histogram indicates the values of effective T_D averaged over two experiments. The 3-nt motifs were ranked corresponding to the averaged effective T_D.

for RNases cytotoxic activity is not known yet and presumably includes pathways involving both specific and nonspecific interactions of cytotoxic RNases with cellular components. This in turn suggests the existence of additional targets besides the elements of protein synthesis machinery (25,27). The study of specific and nonspecific binding of binase to ssDNA as well as to dsDNA may

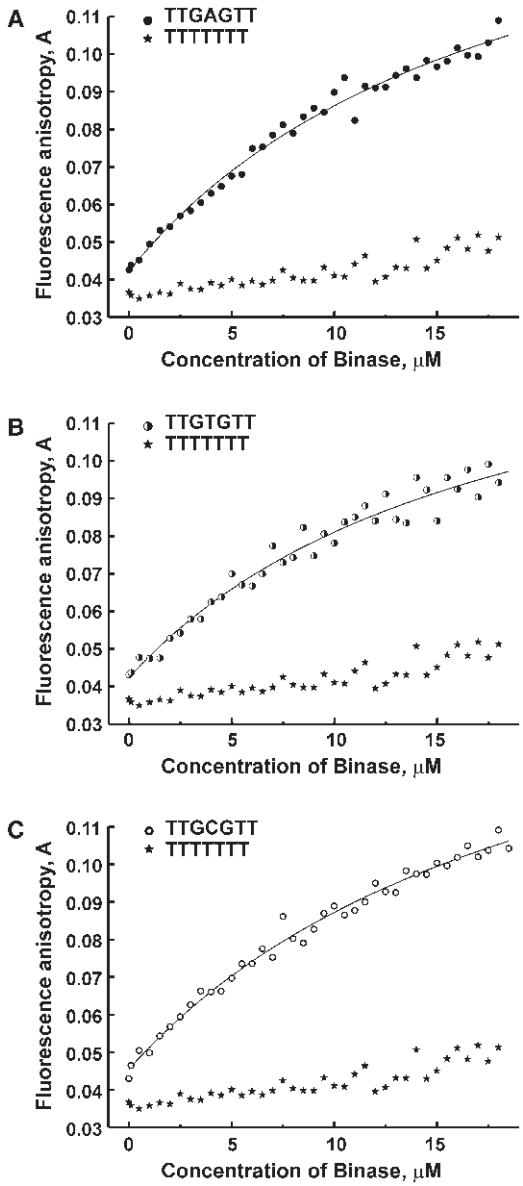

Figure 6. Equilibrium binding of RNase binase to heptadeoxyribonucleotides labeled with Dye-3 monitored using fluorescence anisotropy, $A=(I_{||}-I_{\perp})/(I_{||}+2I_{\perp})$. The plots of A against concentration of binase, C_p, for TTGAGTT (**A**), TTGTGTT (**B**) and TTGCGTT (**C**) are shown in comparison with that for TTTTTTT. Concentration of all oligonucleotides was 10 nM. The sequences of oligonucleotides are shown in the upper left corners. The fitting curves for TTG(A/T/C)GTT oligonucleotides are shown by lines.

shed additional light on the mechanism of cytotoxic action of bacterial ribonucleases.

In this study, we used microchip with oligonucleotides immobilized within 3D hydrogel pads. As it was shown earlier for IMAGE microchips (12,42), immobilized oligonucleotides are evenly distributed within the gel pad volume, are easily accessible because of large pores, are in homogeneous water-like surrounding, and their intermolecular interactions, as well as contacts with solid surface, are negligible. Therefore, the interaction of immobilized short oligonucleotides with the analyzed protein occurs in conditions close to those in solution. This allows to register multiple temperature dissociation curves for protein–oligonucleotide complexes in parallel in equilibrium conditions and to define the affinity of a protein by comparing dissociation temperatures: the higher the dissociation temperature of a given complex, the higher its binding affinity. The only limitation of this approach is the conformational stability of the analyzed protein at high temperature.

In most microarray approaches, the assessment of binding affinities is carried out mostly using the analysis of fluorescence intensities from protein–oligonucleotide complexes formed on microarray at a particular temperature (3–7). In the present study, the analysis of dissociation curves allowed determining an optimal temperature, at which comparison of fluorescence intensities from protein–oligonucleotide complexes on the microchip under protein solution can provide the same assessment of binding specificity as the analysis of dissociation temperatures.

The generic hexamer oligonucleotide platform used in this work is primarily aimed at the study of sequence-specificity of ligands and proteins binding to ssDNA, particularly of proteins whose active sites bind relatively short stretches of DNA. Such microchips may be used for the ranking of complete combinatorial turnover of binding sequences in protein–DNA complexes and inference of specific binding motifs.

SUPPLEMENTARY DATA

Supplementary Data are available at NAR Online.

ACKNOWLEDGEMENTS

The authors are very thankful to Dr Yakovlev G.I. for RNase binase kindly provided for this investigation and helpful discussions. We wish to thank Dr I. Udalova, Kennedy Institute of Rheumatology, Imperial College (London) for fruitful discussions and valuable comments. The assistance of Health Front Line, Ltd. (Champaign, IL) in the preparation of this article for publication is appreciated. This research was supported by International Association for the Promotion of Cooperation with Scientists from the New Independent States of the former Soviet Union (INTAS YSF 04-83-3841). Funding to pay the Open Access publication charges for this article was provided by INTAS.

Conflict of interest statement. None declared.

REFERENCES

1. Bulyk,M.L. (2006) DNA microarray technologies for measuring protein-DNA interactions. *Curr. Opin. Biotechnol.*, **17**, 422–430.
2. Bulyk,M.L. (2006) Analysis of sequence specificities of DNA-binding proteins with protein binding microarrays. *Methods Enzymol.*, **410**, 279–299.
3. Bulyk,M.L. (2007) Protein binding microarrays for the characterization of DNA-protein interactions. *Adv. Biochem. Eng. Biotechnol.*, **104**, 65–85.
4. Field,S., Udalova,I. and Ragoussis,J. (2007) Accuracy and reproducibility of protein-DNA microarray technology. *Adv. Biochem. Eng. Biotechnol.*, **104**, 87–110.

5. Warren,C.L., Kratochvil,N.C., Hauschild,K.E., Foister,S., Brezinski,M.L., Dervan,P.B., Phillips,G.N. Jr. and Ansari,A.Z. (2006) Defining the sequence-recognition profile of DNA-binding molecules. *Proc. Natl Acad. Sci.*, **103**, 867–872.
6. Berger,M.F., Philippakis,A.A., Qureshi,A.M., He,F.S., Estep,P.W. III. and Bulyk,M.L. (2006) Compact, universal DNA microarrays to comprehensively determine transcription-factor binding site specificities. *Nat. Biotechnol.*, **24**, 1429–1435.
7. Morgan,H.P., Estibeiro,P., Wear,M.A., Max,K.E., Heinemann,U., Cubeddu,L., Gallagher,M.P., Sadler,P.J. and Walkinshaw,M.D. (2007) Sequence specificity of single-stranded DNA-binding proteins: a novel DNA microarray approach. *Nucleic Acids Res.*, **35**, e75.
8. Drobyshev,A.L., Zasedatelev,A.S., Yershov,G.M. and Mirzabekov,A.D. (1999) Massive parallel analysis of DNA-Hoechst 33258 binding specificity with a generic oligodeoxyribonucleotide microchip. *Nucleic Acids Res.*, **27**, 4100–4105.
9. Krylov,A.S., Zasedateleva,O.A., Prokopenko,D.V., Rouvière-Yaniv,J. and Mirzabekov,A.D. (2001) Massive parallel analysis of the binding specificity of histone-like protein HU to single and double-stranded DNA with generic oligodeoxyribonucleotide microchips. *Nucleic Acids Res.*, **29**, 2654–2660.
10. Zasedateleva,O.A., Krylov,A.S., Prokopenko,D.V., Skabkin,M.A., Ovchinnikov,L.P., Kolchinsky,A. and Mirzabekov,A.D. (2002) Specificity of mammalian Y-box binding protein p50 in interaction with ss- and dsDNA analyzed with generic oligonucleotide microchip. *J. Mol. Biol.*, **324**, 73–87.
11. Chechetkin,V.R., Prokopenko,D.V., Zasedateleva,O.A., Gitelson,G.I., Lomakin,E.S., Livshits,M.A., Malinina,L., Turygin,A.Y., Krylov,A.S. and Mirzabekov,A.D. (2003) Analysis of binding specificity of disulfide bonded dimeric λ-cro V55C protein with generic hexamer oligonucleotide microchip. *J. Biomol. Struct. Dyn.*, **21**, 425–434.
12. Rubina,A.Y., Pan'kov,S.V., Dementieva,E.I., Pen'kov,D.N., Butygin,A.V., Vasiliskov,V.A, Chudinov,A.V., Mikheikin,A.L., Mikhailovich,V.M. and Mirzabekov,A.D. (2004) Hydrogel drop microchips with immobilized DNA: properties and methods for large-scale production. *Anal. Biochem.*, **325**, 92–106.
13. Condon,C. and Putzer,H. (2002) The phylogenetic distribution of bacterial ribonucleases. *Nucleic Acids Res.*, **30**, 5339–5346.
14. Hill,Ch., Dodson,G., Heinemann,U., Saenger,W., Mitsui,Y., Nakamura,K., Borisov,S., Tischenko,G., Polyakov,K. and Pavlovsky,S. (1983) The structural and sequence homology of a family of microbial ribonucleases. *Trends Biochem. Sci.*, **8**, 364–369.
15. Bulgakova,R.S., Leschinskaya,I.B., Balaban,N.P. and Egorova,G.S. (1974) Some biochemical properties of highly purified extracellular RNase from *Bac. Interme dius*. *Biokhimiya*, **39**, 299–302.
16. Aphanasenko,G.A., Dudkin,S.M., Kaminir,L.B., Leshchinskaya,I.B. and Severin,E.S. (1979) Primary structure of ribonuclease from Bacillus intermedius 7P. *FEBS Lett.*, **97**, 77–80.
17. Sevcik,J., Sanishvili,R.G., Pavlovsky,A.G. and Polyakov,K.M. (1990) Comparison of active sites of some microbial ribonucleases: structural basis for guanylic specificity. *Trends Biochem. Sci.*, **15**, 158–162.
18. Polyakov,K.M., Lebedev,A.A., Okorokov,A.L., Panov,K.I., Schulga,A.A., Pavlovsky,A.G., Karpeisky,M.Y and Dodson,G.G. (2002) The structure of substrate-free microbial ribonuclease binase and of its complexes with 3′GMP and sulfate ions. *Acta. Crystallogr. D Biol. Crystallogr.*, **58 (Pt 5)**, 744–750.
19. Watanabe,H., Ando,E., Ohgi,K. and Irie,M. (1985) The subsite structures of guanine-specific ribonucleases and a guanine-preferential ribonuclease. Cleavage of oligoinosinic acids and poly I. *J. Biochem.*, **98**, 1239–1245.
20. Day,A.G., Parsonage,D., Ebel,S., Brown,T. and Fersht,A.R. (1992) Barnase has subsites that give rise to large rate enhancements. *Biochemistry*, **31**, 6390–6395.
21. Baudet,S. and Janin,J. (1991) Crystal structure of a barnase-d(GpC) complex at 1.9 A resolution. *J. Mol. Biol.*, **219**, 123–132.
22. Buckle,A.M. and Fersht,A.R. (1994) Subsite binding in an RNase: structure of a barnase-tetranucleotide complex at 1.76-A resolution. *Biochemistry*, **33**, 1644–1653.
23. Fontecilla-Camps,J.C., de Llorens,R., le Du,M.H. and Cuchillo,C.M. (1994) Crystal structure of ribonuclease A.d(ApTpApApG) complex. Direct evidence for extended substrate recognition. *J. Biol. Chem.*, **269**, 21526–21531.
24. Wang,L., Pang,Y., Holder,T., Brender,J.R., Kurochkin,A.V. and Zuiderweg,E.R. (2001) Functional dynamics in the active site of the ribonuclease binase. *Proc. Natl Acad. Sci. USA*, **98**, 7684–7689.
25. Leland,P.A. and Raines,R.T. (2001) Cancer chemotherapy – ribonucleases to the rescue. *Chem. Biol.*, **8**, 405–413.
26. Leland,P.A., Staniszewski,K.E., Kim,B.M. and Raines,RT. (2001) Endowing human pancreatic ribonuclease with toxicity for cancer cells. *J. Biol. Chem.*, **276**, 43095–43102.
27. Makarov,A.A. and Ilinskaya,O.N. (2003) Cytotoxic ribonucleases: molecular weapons and their targets. *FEBS Lett.*, **540**, 15–20.
28. Cantor,C.R., Warshaw,M.M. and Shapiro,H. (1970) Oligonucleotide interactions. 3. Circular dichroism studies of the conformation of deoxyoligonucleotides. *Biopolymers*, **9**, 1059–1077.
29. Mikheikin,A.L., Chudinov,A.V., Iaroshchuk,A.I., Rubina,A.I., Pan′kov,S.V., Krylov,A.S., Zasedatelev,A.S. and Mirzabekov,A.D. (2003) A fluorescent dye with low specificity to nucleotide sequences of DNA: use for assessing the quantity of oligonucleotides, immobilized in cells of biological microchips. *Mol. Biol.*, **37**, 1061–1070.
30. Golubenko,I.A., Balaban,N.P., Leshchinskaia,I.B., Volkova,T.I., Kleiner,G.I., Chepurnova,N.K., Aphanasenko,G.A. and Dudkin,S.M. (1979) Ribonuclease of *Bacillus intermedius* 7 P. Purification by chromatography on phosphocellulose and several characteristics of the homogeneous enzyme. *Biokhimiia*, **44**, 640–648.
31. Schulga,A., Kurbanov,F., Kirpichnikov,M., Protasevich,I., Lobachov,V., Ranjbar,B., Chekhov,V., Polyakov,K., Engelborghs,Y. and Makarov,A. (1998) Comparative study of binase and barnase: experience in chimeric ribonucleases. *Protein Eng.*, **11**, 775–782.
32. Hermanson,G.T. (1996) Amine-reactive fluorescein derivatives. Texas Red sulfonyl chloride. In *Bioconjugate Techniques*. Academic Press, San Diego, pp. 324–326.
33. Zubtsov,D.A., Ivanov,S.M., Rubina,A.Y., Dementieva,E.I., Chechetkin,V.R. and Zasedatelev,A.S. (2006) Effect of mixing on reaction-diffusion kinetics for protein hydrogel-based microchips. *J. Biotechnol.*, **122**, 16–27.
34. Datta,K. and LiCata,V.J. (2003) Thermodynamics of the binding of Thermus aquaticus DNA polymerase to primed-template DNA. *Nucleic Acids Res.*, **31**, 5590–5597.
35. Yakovlev,G.I., Moiseyev,G.P, Protasevich,I.I., Ranjbar,B., Bocharov,A.L., Kirpichnikov,M.P., Gilli,R.M., Briand,C.M., Hartley,R.W. and Makarov,A.A. (1995) Dissociation constants and thermal stability of complexes of Bacillus intermedius RNase and the protein inhibitor of Bacillus amyloliquefaciens RNase. *FEBS Lett.*, **366**, 156–158.
36. Yakovlev,G.I., Chepurnova,N.K., Moiseev,G.P., Bocharov,A.I. and Lopatnev,S.V. (1987) Specificity of the *Bacillus intermedis* 7P RNase in reaction of polynucleotide cleavage. *Bioorganicheskaya Khimiya*, **13**, 338–343.
37. Singer,M. and Berg,P. (1991) *Genes & Genomes. A changing Perspective*. University Science Books, Mill Valley, California. Ch. 4.1.
38. Hahnen,E., Znamenskaya,L., Koczan,D., Leshchinskaya,I. and Hobom,G. (2000) A novel secreted ribonuclease from *Bacillus intermedis*: gene structure and regulatory control. *Mol. Gen. Genet.*, **263**, 571–580.
39. Kim,J.S., Soucek,J., Matousek,J. and Raines,R.T. (1995) Mechanism of ribonuclease cytotoxicity. *J. Biol. Chem.*, **270**, 31097–31102.
40. Ilinskaya,O., Decker,K., Koschinski,A., Dreyer,F. and Repp,H. (2001) *Bacillus intermedis* ribonuclease as inhibitor of cell proliferation and membrane current. *Toxicology*, **156**, 101–107.
41. Il'inskaia,O.N. and Makarov,A.A. (2005) Why ribonucleases cause death of cancer cells. *Mol. Biol.* (Moscow, in Russian), **39**, 3–13.
42. Rubina,A.Y., Kolchinsky,A., Makarov,A.A. and Zasedatelev,A.S. (2008) Why 3-D? Gel-based microarrays in proteomics. *Proteomics*, **8**, 817–831.